


RESEARCH ARTICLE

Mic60 is essential to maintain mitochondrial integrity and to prevent encephalomyopathy

Tingting Dong^{1,2} | Zai-Qiang Zhang³ | Li-Hong Sun⁴ | Weilong Zhang⁵ | Zhaohui Zhu⁶ | Lin Lin¹ | Lin Yang¹ | An Lv⁴ | Chunying Liu⁴ | Qing Li¹ | Rui-Feng Yang⁷ | Xiuru Zhang⁸ | Yamei Niu^{1,9} | Hou-Zao Chen⁷ | De-Pei Liu⁷ | Wei-Min Tong^{1,9} 

¹Department of Pathology, Institute of Basic Medical Sciences Chinese Academy of Medical Science, School of Basic Medicine Peking Union Medical College, Neuroscience Center, Chinese Academy of Medical Sciences, Beijing, 100005, China

²Biobank of Ninth People's Hospital, Shanghai Jiao Tong University School of Medicine, Shanghai, China

³Department of Neurology, Beijing Tiantan Hospital, Capital Medical University, Beijing, China

⁴Center for Experimental Animal Research, Institute of Basic Medical Sciences Chinese Academy of Medical Science, Beijing, 100005, China

⁵State Key Laboratory of Molecular Oncology, National Cancer Center/Cancer Institute and Hospital, Chinese Academy of Medical Sciences, Peking Union Medical College, Beijing, 100021, China

⁶Department of Nuclear Medicine, Peking Union Medical College Hospital (PUMCH), Beijing, China

⁷State Key Laboratory of Medical Molecular Biology, Institute of Basic Medical Sciences Chinese Academy of Medical Sciences (CAMS) & School of Basic Medicine Peking Union Medical College (PUMC), Beijing, China

⁸Department of Pathology, Beijing Tiantan Hospital, Capital Medical University, Beijing, China

⁹Molecular Pathology Research Center, Chinese Academy of Medical Sciences and Peking Union Medical College, Beijing, 100005, China

Correspondence

De-Pei Liu, State Key Laboratory of Medical Molecular Biology, Institute of Basic Medical Sciences Chinese Academy of Medical Sciences (CAMS) & School of Basic Medicine Peking Union Medical College (PUMC), Beijing, China.

Email: liudp@pumc.edu.cn

Wei-Min Tong, Department of Pathology, Institute of Basic Medical Sciences Chinese Academy of Medical Science, School of Basic Medicine Peking Union Medical College, Neuroscience Center, Chinese Academy of Medical Sciences, Beijing 100005, China.

Email: wmtong@ibms.pumc.edu.cn

Funding information

CAMS Initiative for Innovative Medicine, Grant/Award Numbers: 2016-I2M-2-001, 2016-I2M-1-004; Cross disciplinary Research Fund of Shanghai Ninth People's Hospital, Shanghai Jiao Tong university School of Medicine, Grant/Award Number: JYJC202104; National Key R&D Program of China, Grant/Award Numbers: 2019FYA 080703, 2021YFA0804900; National Natural Science

Abstract

Mitochondrial encephalomyopathies (ME) are frequently associated with mutations of mitochondrial DNA, but the pathogenesis of a subset of ME (sME) remains elusive. Here we report that haploinsufficiency of a mitochondrial inner membrane protein, Mic60, causes progressive neurological abnormalities with insulted mitochondrial structure and neuronal loss in mice. In addition, haploinsufficiency of *Mic60* reduces mitochondrial membrane potential and cellular ATP production, increases reactive oxygen species, and alters mitochondrial oxidative phosphorylation complexes in neurons in an age-dependent manner. Moreover, haploinsufficiency of *Mic60* compromises brain glucose intake and oxygen consumption in mice, resembling human ME syndrome. We further discover that MIC60 protein expression declined significantly in human sME, implying that insufficient MIC60 may contribute for pathogenesis of human ME. Notably, systemic administration of antioxidant N-acetylcysteine largely reverses mitochondrial dysfunctions and metabolic disorders in haplo-insufficient *Mic60* mice, also restores neurological abnormal symptom. These results reveal Mic60 is required in the maintenance of mitochondrial integrity and function, and likely a potential therapeutics target for mitochondrial encephalomyopathies.

Tingting Dong and Zai-Qiang Zhang contributed equally to this study.

This is an open access article under the terms of the [Creative Commons Attribution-NonCommercial-NoDerivs](https://creativecommons.org/licenses/by-nc-nd/4.0/) License, which permits use and distribution in any medium, provided the original work is properly cited, the use is non-commercial and no modifications or adaptations are made.

© 2023 The Authors. *Brain Pathology* published by John Wiley & Sons Ltd on behalf of International Society of Neuropathology.

Foundation of China, Grant/Award Numbers: 31471343, 82201275; the Interdisciplinary Program of Shanghai Jiao Tong University, Grant/Award Number: YG2022QN064

KEYWORDS

antioxidant, Mic60, mitochondria, mitochondrial encephalomyopathies, neurodegeneration, reactive oxygen species

1 | INTRODUCTION

Mitochondria are cytoplasmic organelles with outer and inner membranes of all aerobic nucleated cells. The inner mitochondrial membrane is highly folded into the cristae and harbors the respiratory chain complexes of the electron transport chain and ATP synthase [1]. Maintenance of mitochondrial structure and function is particularly important to neurons because its high energy demand only relies on glucose oxidation [2]. Thus, mitochondrial dysfunction can severely compromise neuronal functions and is in turn one of the main causative factors leading to neurodegenerative disorders [3, 4]. Mitochondrial DNA (mtDNA) mutations, by impairing respiratory chain/oxidative phosphorylation (OXPHOS), could affect the organs with a high demand of oxidative metabolism (such as the brain and muscle) and further lead to mitochondrial encephalomyopathies (ME) [5–7]. Because of an impaired energy state, ME may be accompanied with lactic acidosis and stroke-like episodes (MELAS) or myoclonus epilepsy and ragged red fibers (MERRF). However, a subset of ME (sME) was found of no mtDNA mutation, which indicates the presence of other reasons causing mitochondrial dysfunction, such as mutations of energy related nuclear genes [8].

Mic60 (also called Mitofilin or Immt), originally named as heart muscle protein (HMP) [9], is a nuclear gene encoding mitochondrial inner membrane protein ubiquitously expressed in fetal and adult tissues, with the highest expression in muscle and the brain [10]. Mic60 expression was significantly decreased in the brains of fetal Down syndrome as well as Parkinson' disease (PD). [11, 12] As a central component of the mitochondrial contact site and cristae organizing system (MICOS), a large protein complex which comprises MIC60, MIC27/APOOL, MIC26, MIC25/CHCHD6, MIC19/CHCHD3, MIC10, MIC14/CHCHD10, MIC23/APOO and MIC13/QIL1 [13–15], MIC60 is essential for mitochondrial membrane architecture as well as in mitochondrial dynamics [15, 16]. Moreover, Mic60 has physical interaction with the outer membrane proteins including SAMM50 and Metaxin, as well as inner membrane/intermembrane space proteins OPA1 and Hsp70, which are involved in mitochondrial cristae morphology and function [17–22]. In addition, Mic60 was found to interact with a mitochondrial protein DISC1 involved in schizophrenia [23], DNA damage response protein PARP-1 [24], PNKP functioning in mitochondrial DNA (mtDNA) stability [25], and PINK1, a mitochondrial serine/threonine kinase involved in PD [26]. Furthermore, phosphorylation of Mic60 by

PKA and PINK1 is essential in maintaining mitochondrial membrane structures and might be involved in the pathogenesis of Parkinson's disease [27, 28]. Interestingly, all these mitochondrial proteins are involved in a subset of neurodegenerative diseases [16].

In this study, we investigated the potential role of Mic60 in neuronal function by using *Mic60* haploinsufficient mouse model. We found that haploinsufficiency of *Mic60* caused neurological abnormalities with neuronal loss in an age-dependent manner. In addition, haploinsufficiency of *Mic60* altered mitochondrial function, promoted brain glucose intake and oxygen consumption in mice, which resembles human ME. Intriguingly, antioxidant N-acetylcysteine largely reversed mitochondrial dysfunctions and metabolic disorders, as well as neurological disable in heterozygotic *Mic60* mice. Besides haploinsufficiency of *Mic60* induced ME in murine, distinct MIC60 protein expression lessening was observed in human ME. These results revealed an essential role of Mic60 in maintaining mitochondrial function and prevention of neurodegeneration, especially ME.

2 | MATERIALS AND METHODS

2.1 | Clinical information

Based on clinical presentation, magnetic resonance neuroimaging abnormalities, evidence of muscle histopathological, and mitochondrial ultrastructural changes, a subset of eight ME patients (male 6, female 2 from 16 to 79-year-old, median age 39.5 years, out of 57 ME patients screened for mtDNA, without the presence of mtDNA mutations) and four ME patients with mtDNA mutations were enrolled (Table S4) in the Neuromuscular and Genetic Centre, Department of Neurology, Beijing Tiantan Hospital. The subject's consent was obtained according to the Declaration of Helsinki, and Institutional ethical committee approval was obtained.

2.2 | Generation of *Mic60*-deficient mice

A gene trap with an insertion in the third intron of the *Mic60* gene was donated from the Sanger Institute. The ES clone (AW 0256) was injected to generate *Mic60*^{+/-} mice. All mice were maintained in a temperature-controlled barrier facility with a 12-h light/dark cycle and were given free access to food and water in the Center for Experimental Animal Research, IBMS, PUMC/CAMS,

Beijing. All animal experiments were performed according to the guideline of Institutional Animal Care and Use Committee (IACUC) of IBMS/PUMC. *Mic60* genotyping PCR primers are listed as follows:

Primer 1 forward 5'-TTGCTTTGCTGACTGTTC-CACT-3'.

Primer 2 reverse 5'-CTGACCTGAAGATCGTCTCCGT-3'.

Primer 3 forward 5'-AAGCGGTGAAGTGCCTCTGG-3'.

Primer 4 reverse 5'-CGTTAGGGTCAATGCGGGTC-3'.

2.3 | Small animal imaging

For small animal magnetic resonance imaging (micro-MRI), mouse brain MRI was performed on a 7T MRI animal scanner (Varian). For small animal positron emission tomography (microPET) analysis, all mice were examined under overnight fasting status. A total of 7.4 MBq (0.2 mCi) ^{18}F -FDG (PUMCH, CAMS, Beijing) was injected into peritoneal cavity of each mouse. Anesthesia was performed 45 min later with 1.5% isoflurane in combination with O_2 in 2 L/min using a Summit AS-1-000-7 animal anesthesia system. An Inveon microPET system (Siemens) was used and the acquisition procedure lasted for 5 min for each mouse.

2.4 | ROS analysis

The endogenous ROS was measured on unfixed frozen sections from mice through the conversion of dihydroethidium (DHE) to ethidium [29]. ROS generation was visualized using fluorescence microscopy (Zeiss), and analyzed using TissueQuest 5.0 system (Tissue Gnostics GmbH, Austria).

The ROS level in isolated mitochondrial was determined by measuring the fluorescence intensity upon its reaction with 2',7'-dichlorodihydro-fluorescein diacetate (DCF, Molecular Probes, Eugene, OR) [30], and measured with a Cary eclipse fluorescence spectrophotometer (Varian).

2.5 | LC-MS/MS and data analysis

Proteins were prepared from mice cerebella at different ages and lysed in 7 M urea, 2 M thiourea, 50 mM Tris, 50 mM DTE, 1 mM PMSF, 1 mM RNase and 1 mM DNase, followed by digestion with trypsin (1:50) overnight. The samples were analyzed in duplicate by a self-packed RPC18 capillary LC column (75 μm \times 100 mm, 1.9 μm , Michrom Bioresources). The raw data was acquired by LTQ Orbitrap Velos, and followed by

imported into Progenesis LC-MS (v2.6, Nonlinear Dynamics, UK). To integrate MS features with protein identities, MS/MS spectra were exported and searched against the SwissProt mouse database using Mascot (v2.4, Matrix Science). Among all the proteins (about 3000 proteins) with CV <90% detected in all the samples, we discarded those proteins that were not detected in more than half samples, and the left 716 proteins were considered as expressed proteins for downstream analysis. Principle component analysis (PCA) were performed using R stats package. Besides, heatmap analysis was processed to reflect the fold change of 716 proteins between the *Mic60*^{+/-} and *Mic60*^{+/-} cerebella of the four stages. The proteins with log₂ (fold change of the expression values) >1 or <-1 and *p*-value <.05 between the *Mic60*^{+/-} and *Mic60*^{+/-} cerebella were defined as differentially expressed protein at each time point. KEGG pathway enrichment analyses were done with those proteins by KOBAS 3.0 online tool [31, 32].

2.6 | Metabolic analysis

Mitochondrial O_2 consumption in cerebellar neuron under basal conditions was measured with high-resolution respirometer (Oroboros Oxygraph-2k, Oxygraph, Innsbruck, Austria) as described [33]. Whole body real-time metabolic analysis was conducted in a comprehensive laboratory animal monitoring system (CLAMS, Columbus Instruments). Oxygen consumption (VO_2) and carbon dioxide production (VCO_2) were evaluated continuously over a 72-h period³⁹ and presented in units of mL/kg/h and normalized to 25°C and 760 mm Hg. Respiratory quotient (RER) was calculated as the ratio of VCO_2/VO_2 .

3 | RESULTS

3.1 | Haploinsufficiency of *Mic60* accelerates age-dependent behavioral alterations

To evaluate whether *Mic60*-deficiency affects behavioral and pathological changes, we generated a knockout mouse model of *Mic60* by gene trap strategy (Figure S1a-d). After germline transmission, *Mic60* heterozygote (*Mic60*^{+/-}) mice were born normally with Mendelian ratio and showed no significant phenotype at birth compared to wild-type mice. Unexpectedly, no *Mic60* homozygote (*Mic60*^{-/-}) mice were born. Genotyping analysis of staged embryos revealed that no viable *Mic60*^{-/-} embryos were found from embryonic day 10.5 (E10.5) on. Moreover, *Mic60*^{-/-} embryos were much smaller than those of wild-type littermates at E7.5 (Figure S1e), and showed massive apoptosis at E9.5 (Figure S1f), which was also observed in *Mic60*-knockdown cells [22]. These results demonstrated an essential role of *Mic60* for early embryonic development.

Haploinsufficiency of *Mic60* in *Mic60*^{+/-} mice was confirmed by determining its expression at both protein and mRNA levels (Figure 1A,B). Although *Mic60*^{+/-}

mice did not show distinct phenotype at early age, these mice exhibited progressive motor dysfunction as early as 6-month (6m). *Mic60*^{+/-} mice displayed gait changes in

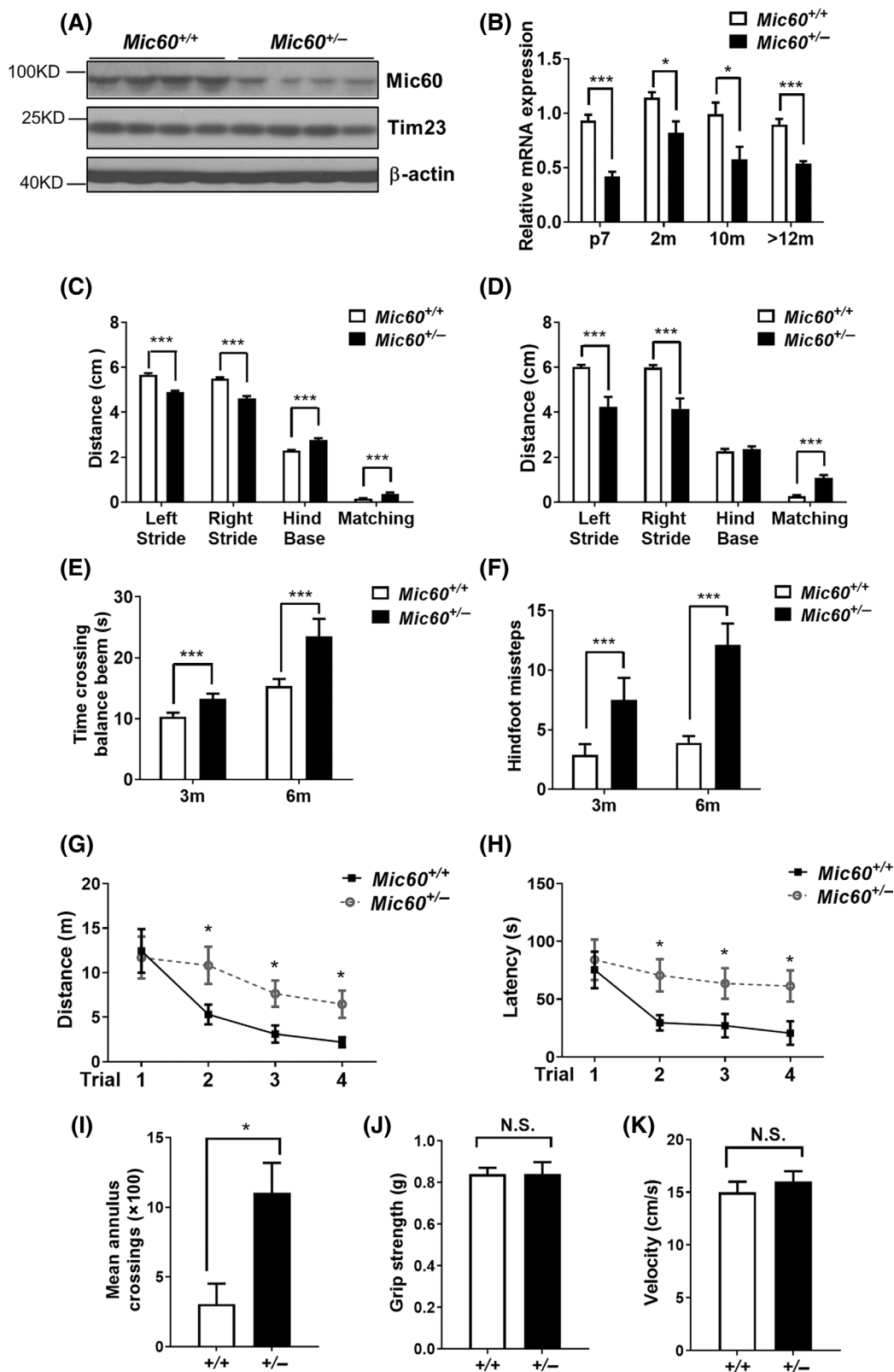


FIGURE 1 Legend on next page.

the left and right stride length by measuring the hind base between right and left paw prints and the matching (Figure S1g). Shorter stride length but increased hind base and matching were observed in *Mic60*^{+/-} mice of 6m and 12m old (Figure 1C,D). *Mic60*^{+/-} mice showed time crossing balance beams and missteps increased at different ages by balance beam test, revealing poor motor balance and coordination (Figure 1E,F). We next performed Morris maze test to further evaluate the coordination and spatial memory ability (Figure S1h). In sharp contrast to wild-type mice, *Mic60*^{+/-} mice showed impaired ability to locate the platform after training, with rotated trace (Figure 1G-I). However, the grip strength (Figure 1J) and velocity (Figure 1K) were equivalent to those of wild-type mice, indicating that abnormal behaviors in *Mic60*^{+/-} mice are likely caused by impaired motor function and coordination, rather than reduced muscle tension or motion speed. These early onset neurological abnormalities in *Mic60*^{+/-} mice suggested haploinsufficiency *Mic60* accelerated neurodegeneration.

3.2 | Insufficient *Mic60* alternates brain structural in mice

To explore the morphological basis of the neurological defects in *Mic60*^{+/-} mice, we then performed brain micro-magnetic resonance imaging analysis (micro-MRI) using paired *Mic60*^{+/-} and wild-type mice. Representative coronal view of T2-weighted micro-MRI images of *Mic60*^{+/-} mice with neurological disorders revealed heterogeneity and partial enlargement of lateral ventricle in *Mic60*^{+/-} mice (Figure 2A, upper panel). The sizes of hippocampus and cerebellum were quantified by calculating the T2 values in sagittal images (Figure 2A, lower panel) followed by ROI analysis (Figure 2B). Compared to wild-type mice, *Mic60*^{+/-} mice displayed a significant reduction in volume of hippocampus, and a trend toward less volume of cerebellum ($p = .0509$, non-parametric Mann-Whitney t -test) (Figure 2B). T2 mapping was carried out to quantify the differences observed in the T2-weighted images. T2 relaxation time showed a significant difference in the regions of hippocampus and cerebellum between the wild-type and *Mic60*^{+/-} mice (Figure 2C), which is similar to the MRI characters of ME patient.

We next performed histological examination of the *Mic60*^{+/-} brains and found a significant loss of cerebellar

Purkinje's cells (Figure 2D, upper panel) in 12m-old mice with typical neurological abnormalities. As *Mic60* may be related with dopamine function [12], we analyzed tyrosine hydroxylase (TH) immunoactivity and observed a marked reduction of dopaminergic neurons in the substantia nigra (SNR) of *Mic60*^{+/-} brain, mirroring pathological changes in PD (Figure 2D, lower panel). In addition, silver staining of *Mic60*^{+/-} brain revealed an increased numbers of neurofibrillary tangles (NFTs) in hippocampus (Figure 2E, upper panel), implying the presence of neurodegenerative changes. To further investigate the role of *Mic60* in mitochondria, we examined mitochondrial morphology in *Mic60*^{+/-} cerebellar neurons by electron microscopy, and found less condensed mitochondria matrix, vacuolation, and partial loss of mitochondrial cristae (Figure 2E, lower panel). Taken together, these pathological changes indicate the presence of mitochondria-associated neuronal disorders in *Mic60*^{+/-} mice.

3.3 | Haploinsufficiency of *Mic60* insults oxidative phosphorylation

To further understand the molecular basis of mitochondria dysfunction in *Mic60*^{+/-} brain, we performed proteomic analysis by using the mouse cerebella of different age groups (P7, 2m, 10m, >12m, respectively) (Figure S2a, Tables S1-S3). Through principal components analysis (PCA), an unsupervised approach designed to group samples based on their similarity in protein expression, we observed that PCA of cerebella from *Mic60*-deficient and -proficient mice were closed at age of P7 based on global DEPs, suggesting a compensatory mitochondrial function in *Mic60*^{+/-} mice (Figure S2b). However, the data sets were moderately separated in the mature *Mic60*^{+/-} mice (2m and 10m) and significantly separated in the phenotypic (>12m) group, implying a compromised mitochondrial function and the onset of ME in the aged mice (Figure S2b). In total, 545 differentially expressed proteins (DEPs) were identified out of ~3000 proteins detected. There is the equal number of DEPs for down- and upregulated at P7. As the age grows, more of the DEPs were downregulated in the *Mic60*^{+/-} mice with apparent neurological abnormalities (Figure S2c). KEGG pathway analysis of all the DEPs revealed 10 most significant pathways in each group (Figure 2F). Strikingly, the top four

FIGURE 1 Haploinsufficiency of *Mic60* caused progressive defects in neuronal functions. (A) Level of *Mic60* protein in the cerebella of *Mic60*^{+/-} mice compared to those in the control mice at P7. Mitochondrial inner membrane protein Tim23 and β -actin were used as internal control. (B) Relative expression of *Mic60* mRNA in mice cerebella at P7, 2 month (2m), 10m, and >12m mice. $n = 5$. (C and D) Gait analysis of wild type and *Mic60*^{+/-} mice. Strides, hind base and matching were measured in mice at 6m (C) and 12m (D). $n = 10$. (E and F) Balance beam tests of wild type and *Mic60*^{+/-} mice. Time durations (s) (E) to cross the beam were recorded for mice of 3m and 6m. Frequencies of hindfeet missteps (F) in mice of 3m and 6m old ($n = 21$). Morris water maze tests for distance (G), latency (H) and mean annulus crossing (I) of mice at 12m ($n = 11$). (J) Grip strength test of 12m-old mice ($n = 12$). (K) Analysis of mean mice velocity (expressed in cm/s) ($n = 12$). White bar, *Mic60*^{+/+}; black bar, *Mic60*^{+/-}. Error bars represent standard error of the mean (SEM) in this and all following graphs. * $p < 0.05$, *** $p < 0.001$, N.S., non-significant. (Non-parametric Mann-Whitney t -test for B-F, I-K. Repeated measures two-way ANOVA with Tukey's HSD test for G, H).

pathways affected in *Mic60*-deficient neurons were Huntington's disease (HD), Parkinson's disease (PD), OXPHOS pathways and Alzheimer's disease (AD) (Figure 2F).

Additional pathways for metabolic pathways and carbon metabolism were also compromised in *Mic60*-deficient brains. These six pathways showed similar dynamic

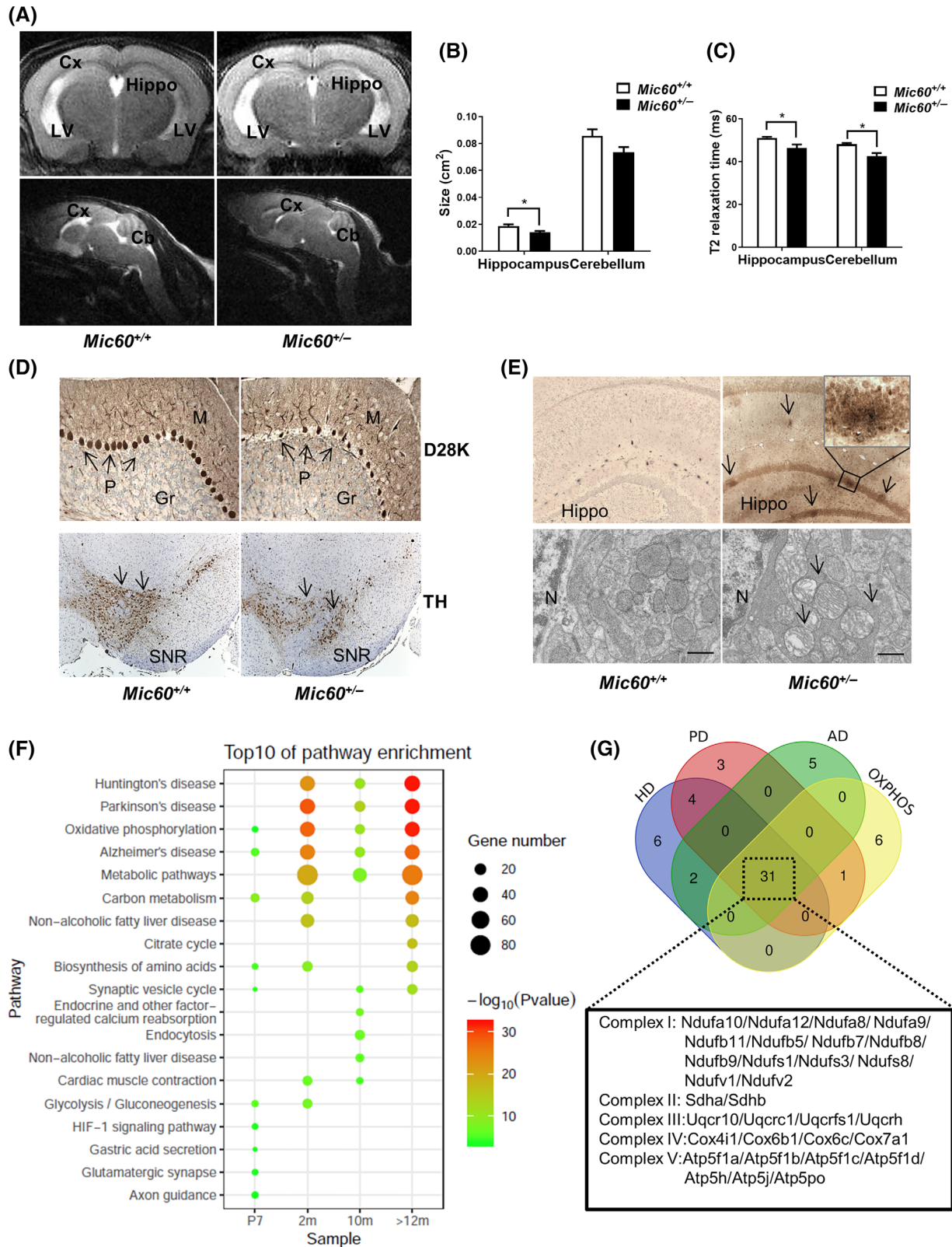


FIGURE 2 Legend on next page.

patterns, throughout the four time points in *Mic60*^{+/-} cerebella. Haploinsufficiency of *Mic60* gradually increased its impact on these six pathways from immature neurons (P7), mature neurons (2m and 10m) to aging neurons (>12m) that associates with the onset of neurological disorders in *Mic60*^{+/-} mice (Figure 2F). Notably, out of 58 DEPs involved in HD, PD, OXPHOS and AD pathways, 31 (53.4%) DEPs shared by all these four pathways are members of complex I, II, III, IV and complex V, which are essential for maintaining mitochondrial stability (Figure 2G). Thus, haploinsufficiency of *Mic60* altered the expression levels of protein components of mitochondrial OXPHOS complexes in neurons that may cause defective mitochondrial respiratory chain integrity, and the dynamic changes of DEPs and associated pathways reveal early molecular events leading to the genesis of ME.

3.4 | Haploinsufficiency of *Mic60* alters mitochondrial function in the murine brain

To explore the mechanism of neuronal disorders in *Mic60*^{+/-} mice, we analyzed haploinsufficiency of *Mic60* affected mitochondrial functions as it is essential for maintaining mitochondrial membrane architecture. However, we found that there was no difference in mtDNA copy number between wild-type and *Mic60*^{+/-} mice (Figure 3A). Because the principal function of mitochondria is ATP synthesis through OXPHOS and brain cells have a high energy demand, we detected significantly impaired OXPHOS function (Figure 3B,C) and ATP generation in *Mic60*^{+/-} brain (Figure 3D), indicating basal mitochondrial oxygen consumption and ATP production levels getting worse while *Mic60* haploinsufficiency. In addition, the *Mic60*^{+/-} brain exhibited a reduction in mitochondrial membrane potential (Figure 3E), suggesting a defective mitochondrial functions in the *Mic60*^{+/-} brain.

ROS are products of a normal cellular metabolism and well-known biomarkers of mitochondrial metabolism [34, 35]. To monitor the consequence of compromised mitochondrial functions in the *Mic60*^{+/-} brain, we analyzed ROS level in brain tissues. Compared to that in

the wild-type mice, enhanced level of ROS was evidenced in *Mic60*-deficient cerebellar neurons (Figure S3a,b). Consequently, *Mic60*^{+/-} cerebellar neurons exhibited high immunoactivity of 8-oxo-2'-deoxyguanosine (8-OHdG) and nitrotyrosine (Figure S3c), which are the major products of DNA and protein oxidation, respectively, implying an active endogenous oxidative stress in the *Mic60*^{+/-} brain.

To test whether *Mic60*^{+/-} mice are sensitive to exogenous DNA damage, postnatal day 7 (P7) mice were subjected to X-ray irradiation. Upon DNA damage, early DNA damage response markers such as phosphorylated 53BP1 and SMC1 foci formation [36] were markedly increased in external granule cell layer (EGL) of proliferating *Mic60*^{+/-} cerebella compared to those in wild-type cerebella (Figure S3d, upper and middle panels). In addition, *Mic60*^{+/-} cerebellar neurons exhibited an increased cell apoptosis after DNA damage (Figure S3d, lower panel). Together, these data imply that *Mic60*-deficient neurons are more sensitive to DNA damage.

3.5 | *Mic60*-deficiency causes metabolic disturbance in murine brain

Accumulating evidence has suggested a strong correlation between metabolic changes and neurodegeneration [37, 38]. As metabolic pathway was significantly affected in *Mic60*-deficient brain based on LC-MS/MS analysis, we next analyzed metabolic changes in heterozygotic *Mic60* mice. As neurons are sensitive to energy supply and glucose is the major energy source to the adult brain under physiological conditions, we first monitored the glucose metabolism in the brains of paired wild-type and *Mic60*^{+/-} mice through ¹⁸F-fluorodeoxyglucose (¹⁸FDG) microPET scanning. A significant higher level of ¹⁸F-FDG uptake was observed in the brain of *Mic60*^{+/-} mice (Figure 3F,G), suggesting an elevated glucose transport in the neurons. This likely reflects an increased anaerobic glycolysis as compensation to disturbed energy metabolism in *Mic60*^{+/-} mice. In addition, age-matched wild-type and *Mic60*^{+/-} mice without (2m and 10m) and with apparent neurological phenotypes (>12m, NDs) were

FIGURE 2 Heterozygotic *Mic60* mice displayed brain structural alterations. (A) Representative MRI image shown in coronal view (upper panel) and sagittal view (lower panel) of *Mic60*^{+/+} and *Mic60*^{+/-} mice at 18m. Cx, cerebral cortex; Hippo, hippocampus; Cb, cerebellum; LV, lateral ventricle. (B) The sizes of hippocampus and cerebella were quantified by calculating the T2 values in sagittal image. The size of hippocampus was measured by mean value of bilateral size in coronal view, and the size of cerebellum was measured by mean value of its size in 1 mm off the median sagittal view. (C) T2 relaxation times were calculated by T2 mapping between the *Mic60*^{+/+} and *Mic60*^{+/-} mice in the regions of hippocampus and cerebella ($n = 5$). White bar, *Mic60*^{+/+}; black bar, *Mic60*^{+/-}, * $p < 0.05$. (Non-parametric Mann-Whitney t -test for B and C). (D) Representative immunostaining images of calbindin-D28K (D28K) in cerebellar Purkinje cells (arrows) and tyrosine hydroxylase (TH, arrows) in substantia nigra (SNR) in mice with apparent neuronal phenotypes (>12m) (Original magnification $\times 40$). M, molecular layer; P, Purkinje cells; Gr, granule cell layer. the scale bar represents 200 μm . (E) Upper panel: Silver staining of neurofibrillary tangle (NFT, arrows, insert) in hippocampus (Hippo) (original magnification $\times 40$). the scale bar represents 200 μm . Lower panel: Electron microscopic view of mitochondria in cerebellar neuron from age-matched mice at 12m. N, nucleus; the scale bar represents 500 nm. (F) KEGG pathway analysis of the differentially expressed proteins (DEPs) in heterozygotic *Mic60* mice cerebella with LC-MS/MS. The top 10 KEGG pathways enriched in DEPs at each time point were shown. Size of the circles indicates the gene numbers, while the color bar represents the $-\log_{10}(p \text{ value})$. (G) A Venn diagram showing the numbers and relationships of DEGs enriched in the HD, PD, OXPHOS, AD pathways in the mice of >12m. Thirty-one proteins involved in mitochondrial complexes formation are enriched in all four pathways.

subjected for Columbus metabolic assays. Notably, *Mic60*^{+/-} mice consumed significantly higher amount of O₂, and produced more CO₂, with higher respiratory exchange ratio (RER, VCO₂/VO₂) than that in wild-type

littermates of 2m and 10m old (Figures 3H and S4), indicating a compensatory response of *Mic60*^{+/-} mice. In contrast, these parameters in *Mic60*^{+/-} mice with phenotype (>12m) were dramatically reduced compared to that in

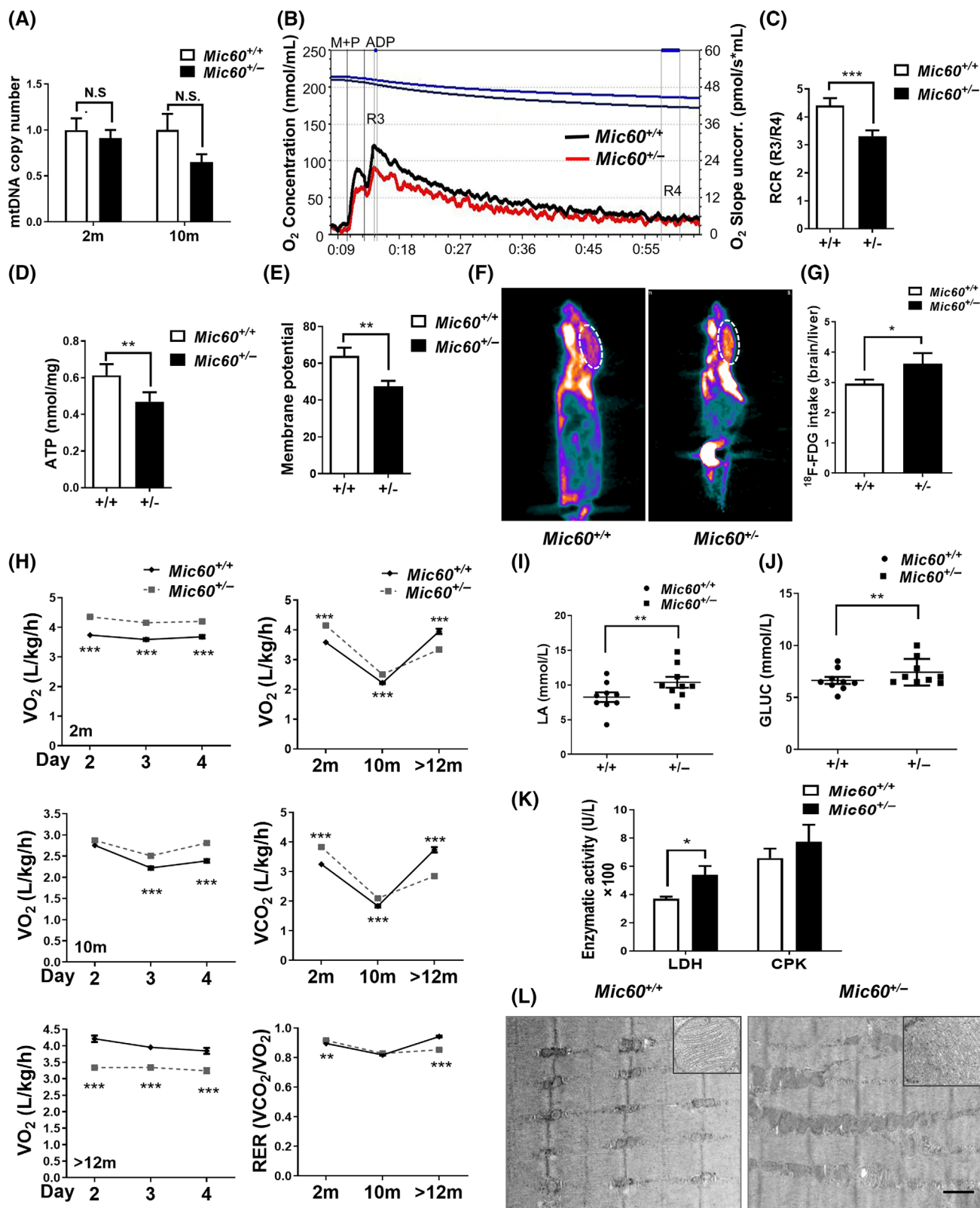


FIGURE 3 Legend on next page.

age-matched wild-type controls (Figure 3H), implying a decompensatory process. Consequently, those *Mic60*^{+/-} mice with phenotype revealed higher levels of serum lactate

(Figure 3I), glucose (Figure 3J), lactate dehydrogenase (LDH), and creatine phosphate kinase (CPK) (Figure 3K). Furthermore, electron microscopic examination of muscle

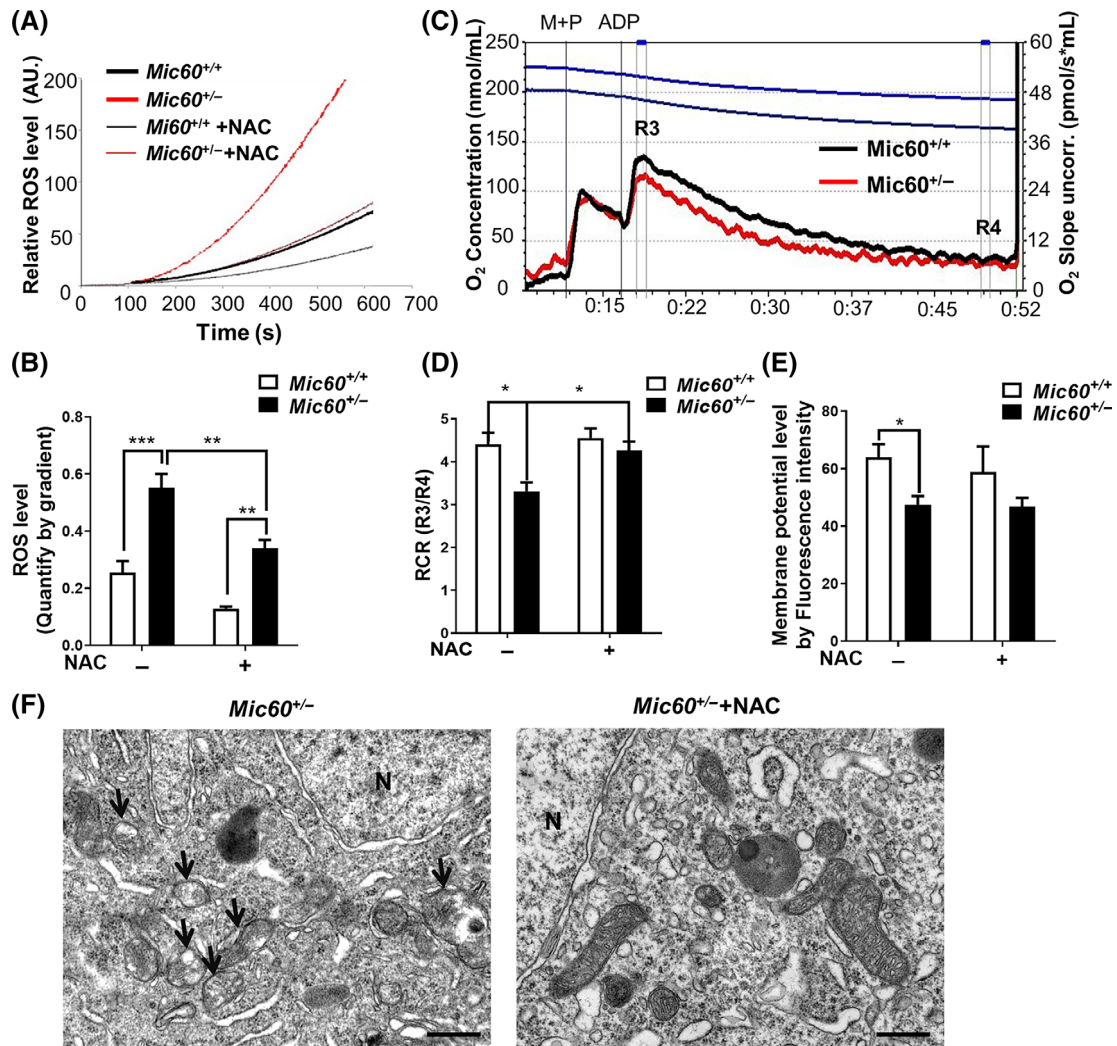


FIGURE 4 Antioxidant treatment largely rescued the defective mitochondrial function. (A) The ROS level in isolated cerebellar mitochondria was measured with DCF in the presence or absence of antioxidant NAC. (B) Quantification of the ROS level in mice at P7 with or without NAC treatment ($n = 6$). (C) Mitochondrial O_2 consumption in cerebellar neuron from 10m-old mice treated with NAC. (D) Quantitative assessment of respiratory control ratio (RCR) by R3/R4 ($n = 9$). (E) Mitochondrial membrane potential was measured in 10m-old cerebella with or without NAC treatment ($n = 6$). (F) Electron microscopic view of mitochondria in cerebellar neuron from 12m-old cerebella with or without NAC treatment. N, nucleus; the scale bar represents 500 nm. White bar, *Mic60*^{+/+}; black bar, *Mic60*^{+/-}; * $p < 0.05$; ** $p < 0.01$; *** $p < 0.001$; N.S., non-significant. Repeated measures two-way ANOVA with Tukey's HSD test for B, D, E.

FIGURE 3 Haploinsufficiency of *Mic60* altered mitochondrial and metabolic function (A) mtDNA copy numbers in mice at 2m and 10m ($n = 6$). (B) Mitochondrial O_2 consumption in cerebellar neuron under basal conditions, following the addition of 10 μ L of M + P (0.8 M malic and 2 M pyruvic acid) and 5 μ L of ADP (20 mM). (C) Respiratory control ratio (RCR) measured by mitochondrial state 3 (R3)/state 4 (R4) ($n = 9$). (D) Haploinsufficiency of *Mic60* led to the decrease of ATP production in mice brains ($n = 11$). (E) Mitochondrial membrane potential measured by fluorescence intensity in mouse cerebella neuron ($n = 6$). * $p < 0.05$; ** $p < 0.01$; *** $p < 0.001$. (Non-parametric Mann-Whitney t -test for A, C-E). (F) Brain microPET image after ^{18}F -FDG intake (dot circle). (G) Quantification of ^{18}F -FDG intake (nCi/cc) in brain normalized by the intake in the liver. (H) Representative 3-day measurement of O_2 consumption was performed at different time points for the reproducibility (left panel) ($n = 4$). Whole body metabolic assays for O_2 consumption (VO_2), CO_2 production (VCO_2), and RER (VCO_2/VO_2) in *Mic60*^{+/+} and *Mic60*^{+/-} mice of different age were summarized in right panel. Blood tests were performed for measurement of lactate (LA) (I), glucose (GLUC) (J), lactate dehydrogenase (LDH) and creatine phosphate kinase (CPK) (K) in *Mic60*^{+/+} and *Mic60*^{+/-} mice at 2 and 10m ($n = 9$). White bar, *Mic60*^{+/+}; black bar, *Mic60*^{+/-}; * $p < 0.05$; ** $p < 0.01$; *** $p < 0.001$. (Non-parametric Mann-Whitney t -test for B, D-F. Repeated measures two-way ANOVA with Tukey's HSD test for C). (L) Electron microscopic examination of mitochondrial density and distribution in the muscle of *Mic60*^{+/+} and *Mic60*^{+/-} mice. The scale bar represents 1 μ m. An enlarged view of mitochondria structure was included.

from *Mic60*^{+/-} mice showed an increased density of mitochondria with relatively normal mitochondrial structure (Figure 3L). These results were in line with the DEPs

analysis of involving metabolic pathways and carbon metabolism, and oxidative phosphorylation in *Mic60*^{+/-} cerebella (Figure 2F), and suggest an elevated anaerobic

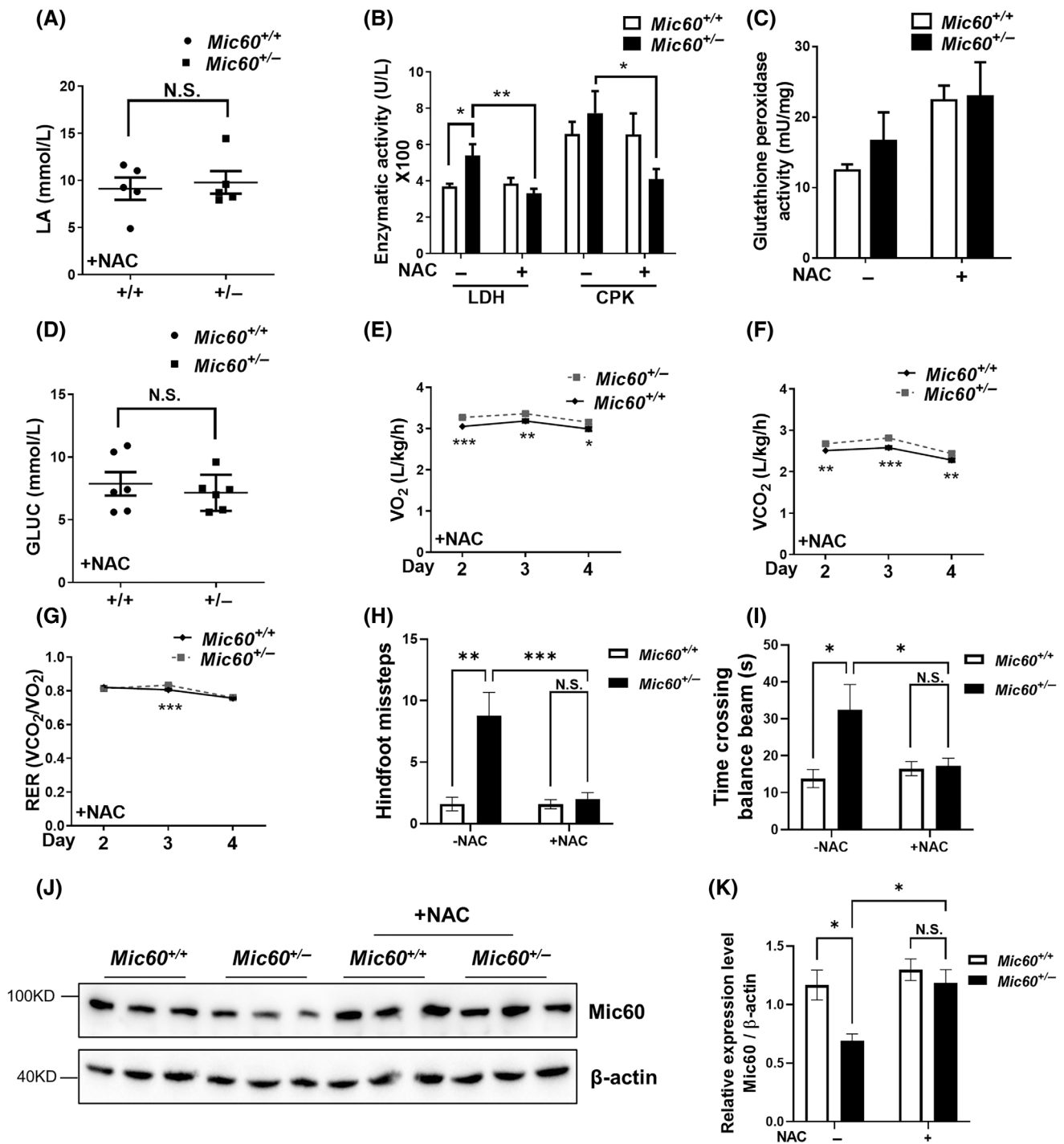


FIGURE 5 Antioxidant treatment largely rescued the metabolic disturbance and behavior dysfunction. Serum tests for lactate (A), glucose (D), lactate dehydrogenase (LDH), and creatine phosphate kinase (CPK) (B) in *Mic60*^{+/+} and *Mic60*^{+/-} mice of 10m-old with NAC treatment ($n = 6$). (C) Glutathione peroxidase activity in mice after treated with NAC for 4 weeks ($n = 5$). Whole body metabolic assays for O₂ consumption (E), CO₂ production (F), and RER (G) in *Mic60*^{+/+} and *Mic60*^{+/-} mice with NAC treatment ($n = 4$). (H, I) Balance beam tests of wild type and *Mic60*^{+/-} mice with NAC treatment. Time durations (s) to cross the beam (h) and frequencies of hindfeet missteps (I) were recorded for mice of 1 year. ($n = 10-14$). Representative immunoblot images (J) and quantification (K) of Mic60 protein level in the cerebella of *Mic60*^{+/-} and *Mic60*^{+/+} mice with/without NAC treatment. β-Actin were used as internal control. ($n = 3$). White bar, *Mic60*^{+/+}; black bar, *Mic60*^{+/-}; * $p < 0.05$; ** $p < 0.01$; *** $p < 0.001$; N.S., non-significant. (Non-parametric Mann-Whitney t -test for A, D. Repeated measures two-way ANOVA with Tukey's HSD test for B, C, E-I).

glycolysis to compensate a disturbance of energy metabolism in *Mic60*^{+/-} mice, resembling human ME.

3.6 | Antioxidant rescues *Mic60* deficiency-induced mitochondria dysfunction

Because oxidative stress can be a cause of energy metabolic disorder, we speculate that reduction in ROS levels may be a therapeutics strategy for ME. N-acetylcysteine (NAC) is an antioxidant nutrition for preventing many diseases including neural disorders [39], which is a potential medication for ME. The peak of ROS in NAC treated *Mic60*^{+/-} cerebellar mitochondria was ~50 AU., reduced to that in wild-type mice, compared to ~200 AU. in untreated mice (Figure 4A). Haploinsufficiency of *Mic60*

increased ROS level in murine cerebella, and NAC administration declined ROS level significantly in *Mic60*^{+/-} mice (Figure 4B). Coincidentally, NAC-treated mitochondria from the *Mic60*^{+/-} cerebellar neurons exhibited an elevated O₂ consumption and mitochondrial membrane potential (Figure 4C–E). Compared to vacuolation and partial loss of mitochondrial cristae in untreated *Mic60*^{+/-} cerebellar neurons, we do not observe abnormal mitochondria ultrastructure after NAC treatment (Figure 4F).

3.7 | Behavior dysfunction is restored by NAC in *Mic60* haploinsufficiency mice

To compare long-term effect of NAC against ME, we supplied NAC for 1 year. In addition, administration of

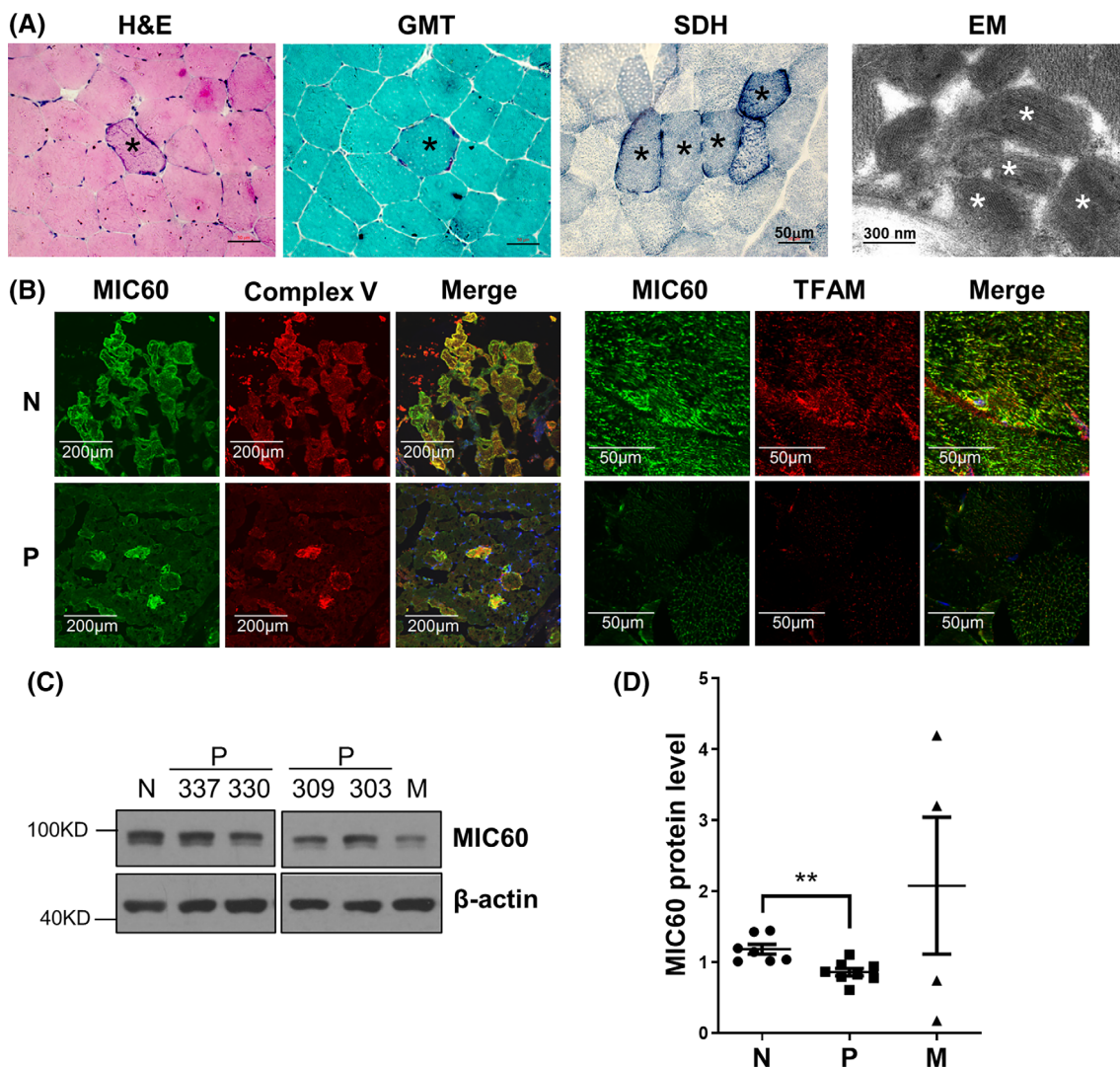


FIGURE 6 Down-expression of MIC60 in human ME in the absence of mtDNA mutation. (A) Representative histological analysis of mitochondrial encephalomyopathies without mtDNA mutation. Biopsies were subjected for hematoxylin–eosin (H&E), the modified Gomori trichrome (GMT) for ragged-red fibers (RRF), succinate dehydrogenase (SDH), and Electron micrograph (EM) for ragged-blue fibers. (B) Representative immunofluorescence staining of MIC60, mitochondrial complex V and inner membrane protein TFAM. (C) Western blotting of MIC60 protein from representative patients (P337, P330, P309, and P303). (D) Quantification of protein expression of MIC60. ***p* < 0.01. (Non-parametric Mann–Whitney *t*-test). N, control; P, ME patients without mtDNA mutation; M, ME patients with mtDNA mutations. *n* = 7 for N, *n* = 8 for *p*, and *n* = 4 for M.

NAC led to a decrease in the levels of serum glucose, lactate, LDH and CPK in *Mic60*^{+/-} mice (Figure 5A,B). These were likely associated with an elevated glutathione peroxidase activity (Figure 5C). Whole body metabolic assay revealed that administration of NAC decreased O₂ consumption, CO₂ production, and RER in *Mic60*^{+/-} mice (for example, VO₂ at 2m was reduced from 4354 ± 40 to 3270 ± 33 mL/kg/h, Figure 3H, Figure 5E–G). However, NAC-treated *Mic60*^{+/-} mice still had relatively higher metabolic activity when compared to the wild-type mice (Figure 5E–G). After NAC administration, *Mic60*^{+/-} mice showed similar time crossing balance beams and missteps increased at 1 year old by balance beam test compared to their littermate control, revealing improved motor balance and coordination (Figure 5H,I). To determine if antioxidant rescued *Mic60* haploinsufficiency induced impairments by upregulation *Mic60* level directly, we compared *Mic60* expression among NAC treated and control groups. The *Mic60* protein increased distinctly in the cerebella of *Mic60*^{+/-} mice after NAC treatment, to the normal level in *Mic60*^{+/+} groups (Figure 5J,K), demonstrating antioxidant restored *Mic60* haploinsufficiency induced dysfunction by upregulation *Mic60* level. These results implicate that antioxidant NAC could largely reverse those metabolic alterations and neuronal dysfunction in *Mic60*^{+/-} mice.

3.8 | ME is associated with decreased MIC60 in ME patients

According to above results, we found that majority phenotypes of *Mic60*^{+/-} mice were consistent with the symptom of human ME suggest that haploinsufficiency of *Mic60* might act as a potential cause of the disease. Although majority of ME resulted from mutations of mtDNA [40], the pathogenesis of a subset of ME (sME) without mtDNA mutation remains unknown. Because mutations of nuclear genes encoding mitochondria OXPHOS complexes play an important role in mitochondria disorders [41], and *Mic60* serves as a key component of the MICOS, we therefore tested whether MIC60 is involved in the sME. We thus selected eight patients of sME without mtDNA mutation to investigate the possible role of MIC60 (Table S4). These patients with sME were diagnosed based on mosaic ragged red fibers (RRF), ragged blue fibers (RBF), mitochondria proliferation, and crystalloid inclusions in muscle biopsies, in addition to typical neurological and neuroimaging changes (Table S4, Figure 6A).

We then performed immunostaining analysis for MIC60 from muscle biopsies of the sME patients and observed a mosaic or uniform reduction of MIC60 (Figure 6B). In addition, MIC60 colocalized with OXPHOS complex V and mitochondrial transcription factor A (TFAM), and a significant decrease of complex V and TFAM were evidenced (Figure 6B). The reduction of MIC60 protein was further analyzed by Western blotting (Figure 6C,D) in the sME patients. We also included four ME patients with mtDNA

mutations (M) as control, and no conclusive information obtained because of varied level of MIC60 (Figure 6C,D). These results imply that MIC60 may involve in the pathogenesis of sME.

4 | DISCUSSION

Given the importance of *Mic60* in regulating mitochondrial function and mitochondrial dysfunction contributes to several neural diseases, we generated *Mic60*-deficient mice to identify whether *Mic60* contributes to the pathogenesis of neurodegeneration. We found that haploinsufficiency of *Mic60* in mice caused neurological abnormalities with defective mitochondrial structure and function, as well as metabolic disorders, similar to ME patients [1]. Consistently, pathological alterations of sME patients suggested dysfunction of MIC60. Administration of NAC, which enhances mitochondria function, restored neuronal and behavior function. These finding illustrated *Mic60* haploinsufficiency caused mitochondria dysfunction, which could be major etiology and therapeutics for ME.

Through a dynamic DEPs analysis, we discovered that in addition to OXPHOS, haploinsufficiency of *Mic60* mainly affected proteins involved in functional pathways of PD, AD, and HD, implying that they may share similar molecular mechanism with sME. Functional study of *Mic60* may also help us to understand other neurodegenerative disease as well. Notably, 31 DEPs shared in all the four pathways were components of mitochondrial complexes I–V (Figure 2G), implying that altered mitochondrial OXPHOS complexes may play a causal role in the sME. In addition, decreased mitochondrial membrane potential, ATP production (not because of the reduction of ATPase activity, data not shown), and accumulation of ROS in *Mic60*^{+/-} cerebellar neurons (Figure 3) revealed a defective mitochondrial integrity [42]. Although how *Mic60*-deficiency affects expression of mitochondrial OXPHOS remains to be answered, this study provides a potential molecular basis for compromised mitochondrial integrity in inducing a subset of neurodegenerative disorders.

Mitochondria play a vital role in neuronal metabolism, in which OXPHOS is the main source of ATP [1]. Consistent with the KEGG pathway analysis of DEPs (Figure 2), haploinsufficiency of *Mic60* in mice led to metabolic disorders with abnormal O₂ consumption, glucose metabolism, and lactic acidosis, suggesting the importance of *Mic60* in the maintenance of cellular metabolic activity to compensate high energy demand in vivo. This response in *Mic60*^{+/-} mice, however, was compromised during aging, leading to neurological abnormalities reminiscent of neurodegenerative disorders.

We reasoned that haploinsufficiency of *Mic60* may induce leakage of electron transport across the inner membrane leading to accumulation of ROS, and thereby tested the role of antioxidant NAC in *Mic60*^{+/-} mice.

We found that NAC treatment largely restored the changes of mitochondrial membrane potential, and the level of O₂ consumption following ROS reduction in *Mic60*^{+/-} mice. It is likely that altered mitochondrial OXPHOS complexes may be an early response to *Mic60* deficiency. Subsequently, defective OXPHOS and ATP synthesis, accumulation of ROS led to neurodegeneration [1, 43]. In line with this notion, an increased expression of MIC60 has been observed in human cardiac myopathy patients [44], and overexpression of *Mic60* in mice led to cardiac hypertrophy in response to hypertrophic stimuli that associated with a decreased cardiac OXPHOS activity and increased ROS production [45]. Thus, a balanced amount of *Mic60* is crucial for the maintenance of mitochondrial integrity and in suppressing ME.

As majority of phenotypes of *Mic60*^{+/-} mice were fit with the symptom of human ME, we therefore selected muscle biopsies from eight patients of sME without mtDNA mutation and seven normal patients with other diseases which will not affect mitochondrial function. Notably, dramatic decreased expression of MIC60 protein was observed in the sME patients coupled with alterations of OXPHOS complex V and mitochondrial TFAM, indicating *MIC60* correlated to ME. Unfortunately, because of the small sample size of sME patients, and lacks ME animal model, detailed role of MIC60 in sME needs to be further investigated. In addition, we did not find mutation in *Mic60* exons from eight sME patients (data not shown), indicating sME maybe not a hereditary disease.

In summary, the present study suggests a role of MIC60 in the pathogenesis of ME, and haploinsufficiency *Mic60* induced ME in murine. Importantly, defective mitochondrial function and metabolic alterations in heterozygote *Mic60* mice can be largely rescued by administration of NAC, implying a potential application of NAC in the treatment of defective mitochondrial-associated neurodegenerative disorders.

AUTHOR CONTRIBUTIONS

De-Pei Liu and Wei-Min Tong initiated the project. Tingting Dong performed most of the experiments. Zai-Qiang Zhang and Xiuru Zhang performed clinical study. Li-Hong Sun, Rui-Feng Yang, Hou-Zao Chen, and De-Pei Liu generated the *Mic60* knockout mice. Li-Hong Sun and Lin Lin performed human samples analysis. An Lv, Chunying Liu, and Qing Li performed behavior study. Tingting Dong and Zhaohui Zhu performed small animal image analysis. Weilong Zhang and Lin Yang performed bioinformatics analysis. Tingting Dong, Li-Hong Sun, Yamei Niu, and Hou-Zao Chen performed data analysis. Tingting Dong, Yamei Niu, and Wei-Min Tong wrote the manuscript.

ACKNOWLEDGMENTS

We thank Mrs. H. M. Zhao, W. Hao, and Dr. H. X. Cui for their excellent technical assistance in the maintenance of the animal colonies, Dr. H. Sun for the LC-MS/MS

data analysis, Tianjin University of Sport for mitochondrial analysis. We also thank Drs. L. Li, T. Tang, and Z. Zheng for critical reading of the manuscript and valuable comments, and Dr. Q. Chen for Tim23 antibody.

FUNDING INFORMATION

Wei-Min Tong was supported by National Key R&D Program of China (2019FYA080703), the National Natural Science Foundation of China (31471343), and CAMS Initiative for Innovative Medicine (2016-I2M-2-001). De-Pei Liu was supported by National Key R&D Program of China (2021YFA0804900). Yamei Niu was supported by CAMS Initiative for Innovative Medicine (2021-I2M-1-020). Tingting Dong was supported by the National Natural Science Foundation of China (82201275), the Interdisciplinary Program of Shanghai Jiao Tong University (YG2022QN064), and Cross disciplinary Research Fund of Shanghai Ninth People's Hospital, Shanghai Jiao Tong university School of Medicine (JYJC202104).

CONFLICT OF INTEREST STATEMENT

The authors declare no conflicts of interest.

DATA AVAILABILITY STATEMENT

Data sharing is not applicable to this article as no new data were created or analyzed in this study.

ORCID

Wei-Min Tong  <https://orcid.org/0000-0002-6240-0267>

REFERENCES

- DiMauro S, Schon EA. Mitochondrial disorders in the nervous system. *Annu Rev Neurosci*. 2008;31:91–123.
- Nunomura A, Moreira PI, Castellani RJ, Lee HG, Zhu X, Smith MA, et al. Oxidative damage to RNA in aging and neurodegenerative disorders. *Neurotox Res*. 2012;22(3):231–48.
- Burchell VS, Gandhi S, Deas E, Wood NW, Abramov AY, Plun-Favreau H. Targeting mitochondrial dysfunction in neurodegenerative disease: part I. *Expert Opin Ther Targets*. 2010;14(4):369–85.
- Burchell VS, Gandhi S, Deas E, Wood NW, Abramov AY, Plun-Favreau H. Targeting mitochondrial dysfunction in neurodegenerative disease: part II. *Expert Opin Ther Targets*. 2010;14(5):497–511.
- McFarland R, Taylor RW, Turnbull DM. The neurology of mitochondrial DNA disease. *Lancet Neurol*. 2002;1(6):343–51.
- Schapira AH. Mitochondrial diseases. *Lancet*. 2012;379(9828):1825–34.
- Tuppen HA, Blakely EL, Turnbull DM, Taylor RW. Mitochondrial DNA mutations and human disease. *Biochim Biophys Acta*. 2010;1797(2):113–28.
- Chinnery PF. Searching for nuclear-mitochondrial genes. *Trends Genet*. 2003;19(2):60–2.
- Tateo I, Tohoru I, Yukie M, Fumio H, Kazuhiko K, Nobuo T. A novel human gene that is preferentially transcribed in heart muscle. *Gene*. 1994;144(2):301–6.
- Gieffers C, Koriath F, Heimann P, Ungermann C, Frey J. Mitofilin is a transmembrane protein of the inner mitochondrial membrane expressed as two isoforms. *Exp Cell Res*. 1997;232(2):395–9.
- Myung J, Gulesserian T, Fountoulakis M, Lubec G. Deranged hypothetical proteins Rik protein, nit protein 2 and mitochondrial

- inner membrane protein, Mitofilin, in fetal down syndrome brain. *Cell Mol Biol.* 2003;49(5):739.
12. Van Laar VS, Dukas AA, Cascio M, Hastings TG. Proteomic analysis of rat brain mitochondria following exposure to dopamine quinone: implications for Parkinson disease. *Neurobiol Dis.* 2008; 29(3):477–89.
 13. Feng Y, Madungwe NB, Bopassa JC. Mitochondrial inner membrane protein, Mic60/Mitofilin in mammalian organ protection. *J Cell Physiol.* 2019;234(3):3383–93.
 14. Guarani V, McNeill EM, Paulo JA, Huttlin EL, Frohlich F, Gygi SP, et al. QIL1 is a novel mitochondrial protein required for MICOS complex stability and cristae morphology. *Elife.* 2015;4:e06265.
 15. Pfanner N, van der Laan M, Amati P, Capaldi RA, Caudy AA, Chacinska A, et al. Uniform nomenclature for the mitochondrial contact site and cristae organizing system. *J Cell Biol.* 2014;204(7): 1083–6.
 16. Zerbes RM, van der Klei IJ, Veenhuis M, Pfanner N, van der Laan M, Bohnert M. Mitofilin complexes: conserved organizers of mitochondrial membrane architecture. *Biol Chem.* 2012;393(11): 1247–61.
 17. Darshi M, Mendiola VL, Mackey MR, Murphy AN, Koller A, Perkins GA, et al. ChChd3, an inner mitochondrial membrane protein, is essential for maintaining crista integrity and mitochondrial function. *J Biol Chem.* 2011;286(4):2918–32.
 18. John GB, Shang Y, Li L, Renken C, Mannella CA, Selker JM, et al. The mitochondrial inner membrane protein Mitofilin controls cristae morphology. *Mol Biol Cell.* 2005;16(3):1543–54.
 19. Ott C, Ross K, Straub S, Thiede B, Gotz M, Goosmann C, et al. Sam50 functions in mitochondrial intermembrane space bridging and biogenesis of respiratory complexes. *Mol Cell Biol.* 2012; 32(6):1173–88.
 20. von der Malsburg K, Müller JM, Bohnert M, Oeljeklaus S, Kwiatkowska P, Becker T, et al. Dual role of Mitofilin in mitochondrial membrane organization and protein biogenesis. *Dev Cell.* 2011;21(4):694–707.
 21. Xie J, Marusich MF, Souda P, Whitelegge J, Capaldi RA. The mitochondrial inner membrane protein Mitofilin exists as a complex with SAM50, metaxins 1 and 2, coiled-coil-helix coiled-coil-helix domain-containing protein 3 and 6 and DnaJC11. *FEBS Lett.* 2007;581(18):3545–9.
 22. Yang RF, Zhao GW, Liang ST, Zhang Y, Sun LH, Chen HZ, et al. Mitofilin regulates cytochrome c release during apoptosis by controlling mitochondrial cristae remodeling. *Biochem Biophys Res Commun.* 2012;428(1):93–8.
 23. Park YU, Jeong J, Lee H, Mun JY, Kim JH, Lee JS, et al. Disrupted-in-schizophrenia 1 (DISC1) plays essential roles in mitochondria in collaboration with Mitofilin. *Proc Natl Acad Sci U S A.* 2010;107(41):17785–90.
 24. Rossi MN, Carbone M, Mostocotto C, Mancone C, Tripodi M, Maione R, et al. Mitochondrial localization of PARP-1 requires interaction with Mitofilin and is involved in the maintenance of mitochondrial DNA integrity. *J Biol Chem.* 2009; 284(46):31616–24.
 25. Tahbaz N, Subedi S, Weinfeld M. Role of polynucleotide kinase/phosphatase in mitochondrial DNA repair. *Nucleic Acids Res.* 2012;40(8):3484–95.
 26. Weihofen A, Thomas KJ, Ostaszewski BL, Cookson MR, Selkoe DJ. Pink1 forms a multiprotein complex with Miro and Milton, linking Pink1 function to mitochondrial trafficking. *Biochemistry.* 2009;48(9):2045–52.
 27. Akabane S, Uno M, Tani N, Shimazaki S, Ebara N, Kato H, et al. PKA regulates PINK1 stability and parkin recruitment to damaged mitochondria through phosphorylation of MIC60. *Mol Cell.* 2016;62(3):371–84.
 28. Tsai PI, Lin CH, Hsieh CH, Papakyrikos AM, Kim MJ, Napolioni V, et al. PINK1 phosphorylates MIC60/Mitofilin to control structural plasticity of mitochondrial crista junctions. *Mol Cell.* 2018;69(5):744–56 e6.
 29. Zielonka J, Kalyanaram B. Hydroethidine- and MitoSOX-derived red fluorescence is not a reliable indicator of intracellular superoxide formation: another inconvenient truth. *Free Radic Biol Med.* 2010;48(8):983–1001.
 30. Wang H, Joseph JA. Quantifying cellular oxidative stress by dichlorofluorescein assay using microplate reader. *Free Radic Biol Med.* 1999;27(5–6):612–6.
 31. Wu J, Mao X, Cai T, Luo J, Wei L. KOBAS server: a web-based platform for automated annotation and pathway identification. *Nucleic Acids Res.* 2006;34:W720–Web Server issue, W724.
 32. Xie C, Mao X, Huang J, Ding Y, Wu J, Dong S, et al. KOBAS 2.0: a web server for annotation and identification of enriched pathways and diseases. *Nucleic Acids Res.* 2011;39(Web Server issue):W316–22.
 33. Gnaiger E. Bioenergetics at low oxygen: dependence of respiration and phosphorylation on oxygen and adenosine diphosphate supply. *Respir Physiol.* 2001;128(3):277–97.
 34. Ott M, Gogvadze V, Orrenius S, Zhivotovsky B. Mitochondria, oxidative stress and cell death. *Apoptosis.* 2007;12(5):913–22.
 35. Scherz-Shouval R, Elazar Z. ROS, mitochondria and the regulation of autophagy. *Trends Cell Biol.* 2007;17(9):422–7.
 36. Lukas J, Lukas C, Bartek J. More than just a focus: the chromatin response to DNA damage and its role in genome integrity maintenance. *Nat Cell Biol.* 2011;13(10):1161–9.
 37. Blandini F, Braunewell KH, Manahan-Vaughan D, Orzi F, Sarti P. Neurodegeneration and energy metabolism: from chemistry to clinics. *Cell Death Differ.* 2004;11(4):479–84.
 38. Procaccini C, Santopaolo M, Faicchia D, Colamatteo A, Formisano L, de Candia P, et al. Role of metabolism in neurodegenerative disorders. *Metabolism.* 2016;65(9):1376–90.
 39. Liu J, Cao L, Chen J, Song S, Lee IH, Quijano C, et al. Bmi1 regulates mitochondrial function and the DNA damage response pathway. *Nature.* 2009;459(7245):387–92.
 40. Zhang ZQ, Niu ST, Liang XH, Jian F, Wang Y. Vascular involvement in the pathogenesis of mitochondrial encephalomyopathies. *Neurol Res.* 2010;32(4):403–8.
 41. Zeviani M, Spinazzola A, Carelli V. Nuclear genes in mitochondrial disorders. *Curr Opin Genet Dev.* 2003;13(3):262–70.
 42. Schon EA, Przedborski S. Mitochondria: the next (neurode)generation. *Neuron.* 2011;70(6):1033–53.
 43. Figueira TR, Barros MH, Camargo AA, Castilho RF, Ferreira JC, Kowaltowski AJ, et al. Mitochondria as a source of reactive oxygen and nitrogen species: from molecular mechanisms to human health. *Antioxid Redox Signal.* 2013;18(16):2029–74.
 44. Marin-Garcia J, Goldenthal MJ, Moe GW. Mitochondrial pathology in cardiac failure. *Cardiovasc Ther Res.* 2001;49(1):17–26.
 45. Zhang Y, Xu J, Luo YX, An XZ, Zhang R, Liu G, et al. Overexpression of Mitofilin in the mouse heart promotes cardiac hypertrophy in response to hypertrophic stimuli. *Antioxid Redox Signal.* 2014;21:1693–707.

SUPPORTING INFORMATION

Additional supporting information can be found online in the Supporting Information section at the end of this article.

How to cite this article: Dong T, Zhang Z-Q, Sun L-H, Zhang W, Zhu Z, Lin L, et al. Mic60 is essential to maintain mitochondrial integrity and to prevent encephalomyopathy. *Brain Pathology.* 2023; 33(4):e13157. <https://doi.org/10.1111/bpa.13157>